P1.81 The Effects of the Quasi-Liquid Layer on Ice Crystal Scattering Calculations

J.C. Hubbert[1],* Sanja B. Manić[2], and Branislav M. Notaroš[2])

[1]National Center for Atmospheric Research, Boulder, CO
[2]Colorado State University, Fort Collins, CO

1. Introduction

It is now well known that there exists a so-called Quasi-Liquid Layer (QLL) on the surface of ice, sometimes referred to as the pre-melting layer (Li and Somorjai 2007; Dash et al. 2006; Prupacher and Klett 1997). The QLL consists of a thin water-like layer that exists at a temperature below the bulk melting point for a given pressure. The thickness of this QLL has been reported as being a few nanometers up to 100 nm and larger. It is thought that the QLL plays an important role in the slipperiness of ice, recrystallization and coarsening of ice grains, regelation (pressure-induced change in freezing), and electrification of thunderclouds. Recently Sazaki et al. (2012) showed direct visualization of the QLL via advanced optical microscopy, which can visualize the individual 0.37-nm-thick elementary steps on ice crystal surfaces. Their results show two distinctly different QLLs existing simultaneously. Work by Furukawa et al. (1987) show that the QLL can have a dielectric constant very close to that of water. This then precipitates the question: can the QLL significantly affect the scattering characteristics of ice crystals in the atmosphere?

The QLL is very thin and until now, its effects on the scattering characteristics of ice crystals has not been investigated. Both the T-matrix and DDA (discreet dipole approximation) techniques have convergence problems with the dimension of ice crystals modeled here. Additionally, the T-matrix methods limited to smooth, rotationally symmetric objects (i.e., prolate and oblate spheroids). Here we use a new higher order method of moments (MoM) to model small columnar ice crystals with large axis ratios (AR).

2. The Model

In order to investigate the QLL, a numerically rigorous full-wave computational electromagnetic technique based on the higher order MoM in the surface integral equation (SIE) formulation (Notaros 2008) is used. According to this method, the external (between QLL and air) and internal (between ice and QLL) dielectric boundary surfaces of a QLL-coated ice crystal are modeled by generalized quadrilateral patches. Electric and magnetic equivalent surface current density vectors over the patches are approximated using hierarchical polynomial vector basis functions. The unknown current-distribution expansion coefficients in the polynomials are determined by a Galerkin-type direct solution to the surface integral equations (SIEs) based on boundary conditions for tangential components of total (incident plus scattered) electric and magnetic fields on all dielectric surfaces in particle models. This modeled has recently been applied to larger precipitation particles and has been compared to the T-matrix and DDA methods (Chobanyan et al. 2015).

We model small ice columns as hexagonal prism shapes with various QLL thicknesses and calculate the polarimetric variables of specific differential phase, K_{dp}, and differential reflectivity, Z_{dr}. Figure 1 shows the crystal shape. The lefthand image shows a 3-dimensional hexagon, the middle image shows the ice crystal column and the righthand image shows the cross section of the hexagon ice crystal with the quasi-liquid layer labeled as water. h is the ice crystal height, w is the width with $b = 2w$. Two axis ratios, 10:1 an 5:1, of columnar ice crystals are modeled:

1. AR=10: $h = 0.5\,\mathrm{mm}$ and $w = 0.05\,\mathrm{mm}$
2. AR=5: $h = 0.5\,\mathrm{mm}$ and $w = 0.1\,\mathrm{mm}$.

The equivalent spherical volume diameters are $D_{eq} = 0.1157\,\mathrm{mm}$ and $D_{eq} = 0.1837\,\mathrm{mm}$, respectively. The QLL has dimensions of $d = 0$ (ice), $d = 50\,\mathrm{nm}$, $d = 100\,\mathrm{nm}$, $d = 500\,\mathrm{nm}$, $d = 5\mu\mathrm{m}$, $d = 20\mu\mathrm{m}$, and pure water. Though unrealistic, the QLL thicknesses $\geq 500\,\mathrm{nm}$ are given for completeness. The frequency is 2.75 GHz (S-band) with dielectric permittivity $er = 3.174$ for ice and $er = 78.31 - j11.33$ for water. From the experimental DSD used in Hubbert et al. (2014), we use N(D)= 150,000 m^{-3} mm^{-1} for AR=5, and 204,000 m^{-3} mm^{-1} for AR=10. The bin width is 0.05 mm for both. Then $n = bwN(D) = 7500\mathrm{m}^{-3}$ for AR=5, and similarly, $n = 10,200\,\mathrm{m}^{-3}$ for AR=10. Of interest are the polarimetric variables, Z_{dr} and K_{dp},

---

*NCAR/EOL, Boulder, Colorado 80307, email: hubbert@ucar.edu which are calculated as

$$Z_{dr} = 10\log_{10}\Big(\frac{|S_{hh}|}{|S_{vv}|}\Big) \tag{1}$$

$$K_{dp} = 10^3\lambda_0 n\Re[F_{hh} - F_{vv}] \tag{2}$$

where S and F are the backscatter and forward scatter amplitudes, and λ_0 is the wavelength.

Tables 1 and 2 show the model results. As the QLL increases, the Z_{dr} and K_{dp} values increase as expected. These absolute values are of less interest and instead we focus on the percent increase in Z_{dr} and K_{dp} for QLL thicknesses of 50 and 100 nm. Such QLL thickness values have been reported in the literature. Table 3 gives the percent increase of Zdr and K_{dp} as compared to solid ice. Significant increases are seen especially for a 10-to-1 axis ratio.

Table 1: 10 to 1 axis ratio. d is the width of the QLL modeled with a dielectric constant of water. $D_{eq} =$ 0.1157mm.

d	$\mathbf{Z_{dr}}$ (dB)	$\mathbf{K_{dp}}$ (deg./km)
0 (ice)	5.633	$0.2335\,10^{-3}$
50nm	6.197	$0.3035\,10^{-3}$
100nm	6.682	$0.3591\,10^{-3}$
500nm	10.905	$0.8529\,10^{-3}$
5μm	20.220	$4.244\,10^{-3}$
20μm	23.584	$6.875\,10^{-3}$
water	23.754	$7.018\,10^{-3}$

Table 2: 5 to 1 axis ratio. d is the width of the QLL modeled with a dielectric constant of water. $D_{eq} =$ 0.1837mm.

d	$\mathbf{Z_{dr}}$ (dB)	$\mathbf{K_{dp}}$ (deg./km)
0 (ice)	4.933	$0.585\,10^{-3}$
50nm	4.956	$0.672\,10^{-3}$
100nm	5.173	$0.752\,10^{-3}$
500nm	8.079	$1.382\,10^{-3}$
5μm	14.38	$5.560\,10^{-3}$
20μm	17.23	$9.239\,10^{-3}$
water	17.89	$10.340\,10^{-3}$

Table 3: The percent increase in Z_{dr} and K_{dp} as compared to solid ice.

AR	5:1		10:1	
QLL (nm)	50	100	50	100
Z_{dr} (%)	0.05	4.8	10.0	18.6
K_{dp}(%)	14.9	28.5	30.0	53.8

3. Discussion and Summary

Here we have shown, with a new MoM scattering model, that the QLL on ice crystals could effect the polarimetric variables of Z_{dr} and K_{dp}. It is well know that water layers of various thicknesses on ice particles, e.g. hail, graupel, enhance the scattering characteristics of such particles especially if the size of the particle is in the MIE scattering regime (Herman and Battan 1961). Here we investigated small columnar ice crystals with a major axis dimension of 0.5 mm, with ARs of 5 and 10, and then applied a QLL of 50 and 100 nm. Such small ice crystals can not be modeled with the more traditional T-matrix and DDA (discrete dipole approximation) because of convergence problems. It has been reported that the QLL has a dielectric constant very close to that of water. Thus we have assumed here that the QLL is rather thick and that it can be modeled as water. A one molecular layer of water is about 0.37 nm thick. Under these assumptions, a QLL of 100 nm increases the Z_{dr} and K_{dp} by 28.5% and 53.8%, respectively, over solid ice. Such increases are very significant will affect polarimetric interpretations of the ice phase of storms. More modeling is warranted.

Acknowledgment The National Center for Atmospheric Research is sponsored by the National Science Foundation. Any opinions, findings and conclusions or recommendations expressed in this publication are those of the authors and do not necessarily reflect the views of the National Science Foundation.

References

Chobanyan, E., N. Šekeljić, A. Manić, M. Ilić, V. Bringi, and B. Notaroš, 2015: Efficient and accurate computational electromagnetics approach to precipitation particle scattering analysis based on higher-order method of moments integral equation modeling. *J. Atmos. Oceanic Tech.*, **32**, 1745–17–58.

Dash, J., A. Rempel, and J. Wettlaufer, 2006: The physics of premelted ice and its geophysical consequences. *Rev. of Mod. Physics*, **78**, 695–741.

Furukawa, Y., M. Yamamoyo, and T. Kuroda, 1987: Ellipsometric study of the ice surface structure just below the melting point. *J. de Physique*, **48**, 495–501.

Herman, B. and L. Battan, 1961: Calculations of MIE backscatterng from melting ice spheres. *J. Meteor.*, **18**, 468–478.

Li, Y. and G. Somorjai, 2007: Surface premelting of ice. *J. of Physical Chem.*, **111**, 9,631–9,637.

Notaros, B., 2008: Higher order frequency-domain computational electromagnetics. *IEEE Trans. Antennas and Propag.,*, **56**, 2251–2276, special Issue on Large and Multiscale Computational Electromagnetics,.

Prupacher, H. and J. Klett, 1997: *Microphysics of Clouds and Precipitation*. Kluwer Acad., Dordrecht, Netherlands, 954 pp.

Sazaki, G., S. Zepeda, S. Nakatsubo, E. Yokoyama, and Y. Furukawa, 2012: Quasi-liquid layers on ice crystal surfaces are made up of two different phases. *Proc. Natl Acad. Sci. USA*, **109**, 1052–1055.

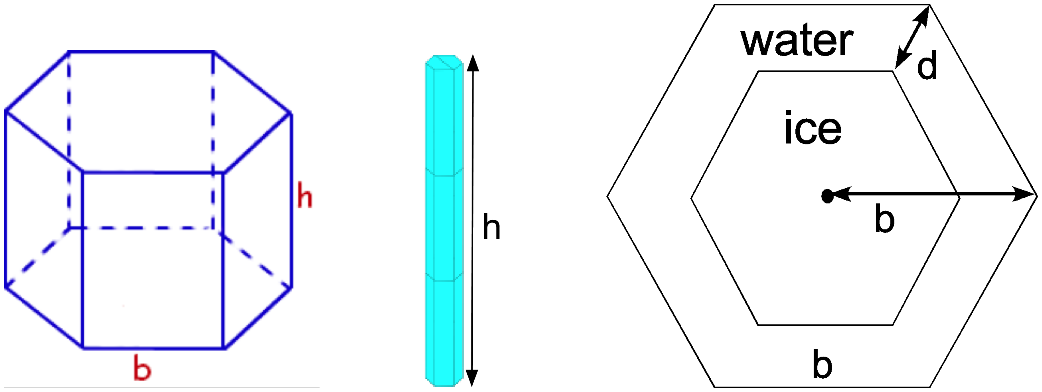

Figure 1: *The modeled ice crystal.*